What is the stiffness of a bent book?

– Supplemental Information –

S. Poincloux, T. Chen, B. Audoly, P. Reis

S.I. Experimental reproducibility

In Fig. S1(a), we present a photograph of the full experimental apparatus described in the main text. This set-up provides highly reproducible mechanical response of the stacks upon multiple loading cycles and shuffling of the layers. This reproducibility is highlighted in Fig. S1(b) where we show the raw force-deflection curves $F_2(w_\circ)$ for a stack with $n = 40$ plates. The stack is bent cyclically, while gardually incrementing the maximum deflection $w_\circ^{\max}$ within the range $6.5 \leq w_\circ^{\max}\,[\mathrm{mm}] \leq 65$, in steps of 6.5 mm at each cycle. The experimental test is repeated three times (represented by the three different color in Fig. S1(b), while maintaining the same number of layers but shuffling them in-between the experiments. For each cycle and for each experimental run, the data overlaps, attesting the reproducibility of our experimental measurements.

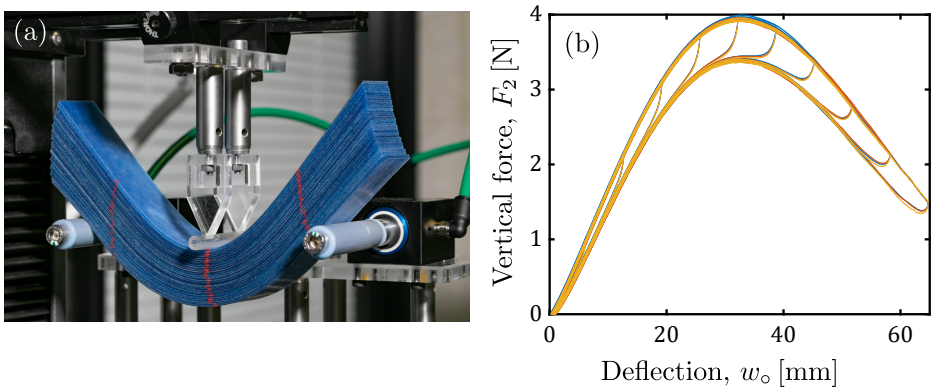

Supplementary Figure S1. (a) Picture of the experimental set-up (photo taken by Alain Herzog). (b) Vertical force against deflection curve $F_2(w_\circ)$ for $n = 40$. At each cycle, $w_\circ^{\max}$ is incrementally increased by 6.5 mm from 6.5 mm to 65 mm ($a = 65$ mm). The three colors represent three different tests with the stack shuffled in-between. Both loading and unloading curves are highly reproducible.

S.II. Geometry and energy of the reduced model for the stack

Kinematics of the stack: Consider a reference inextensible curve $\boldsymbol{x}_{\mathrm{bb}}(S) = x_1(S)\boldsymbol{e_1} + x_2(S)\boldsymbol{e_2}$ in the plane, and its tangent

$$\boldsymbol{t}(S) = \frac{\mathrm{d}\boldsymbol{x}}{\mathrm{d}S} \tag{S1}$$

as well as the normal $\boldsymbol{n}(S)$; see Fig. 2(c) of the main text and Fig. S2(a) for schematic diagrams. The curvature is $\kappa = \mathrm{d}\theta/\mathrm{d}S$ with θ as the angle between $\boldsymbol{t}$ and the horizontal axis. The curve with offset $\tilde{\boldsymbol{x}}(S, y)$ is defined by the non-normal parametrization

$$S \mapsto \tilde{\boldsymbol{x}_{\mathrm{bb}}}(S, y) = \boldsymbol{x}(S) + y\boldsymbol{n}(S). \tag{S2}$$

The arclength $\tilde{S}$ on the offset curve satisfies

$$\mathrm{d}\tilde{S} = |\mathrm{d}\tilde{\boldsymbol{x}_{\mathrm{bb}}}| = |\boldsymbol{t}\mathrm{d}S + y\mathrm{d}\boldsymbol{n}| = (1 - y\kappa)\mathrm{d}S. \tag{S3}$$

We always assume $|y\kappa| < 1$ (no cusp). The offset curves remain parallel to the centerline $\boldsymbol{x}$. The tangent to the offset curve at $\tilde{\boldsymbol{x}}(S, y)$ is parallel to $\boldsymbol{t}(S)$. As a result, the curvature of the offset curve reads

$$\tilde{\kappa} = \frac{\mathrm{d}\theta}{\mathrm{d}\tilde{S}} = \frac{\kappa}{\mathrm{d}\tilde{S}/\mathrm{d}S} = \kappa \cdot (1 - y\kappa)^{-1}. \tag{S4}$$

Energy of the stack: The contribution to the bending energy density $\tilde{\mathcal{E}}$ arising from the 'sector' spanned by $\mathrm{d}S$ reads

$$\tilde{\mathcal{E}}\mathrm{d}S = \int_{-\frac{nh}{2}}^{+\frac{nh}{2}} \frac{\mathrm{d}y}{h} \frac{B_1}{2} \tilde{\kappa}^2 \mathrm{d}\tilde{S} = \int_{-\frac{nh}{2}}^{+\frac{nh}{2}} \frac{\mathrm{d}y}{h} \frac{B_1}{2} \kappa^2 \cdot (1 - y\kappa)^{-1} \mathrm{d}S = \frac{B_1}{2h} \kappa \ln\left(\frac{1 + \frac{nh\kappa}{2}}{1 - \frac{nh\kappa}{2}}\right) \mathrm{d}S. \tag{S5}$$

This can be rewritten as

$$\tilde{\mathcal{E}}(\kappa) = \frac{B_1}{2h} \kappa \ln\left(\frac{1 + \frac{nh\kappa}{2}}{1 - \frac{nh\kappa}{2}}\right) = \frac{B_1}{nh^2} \varphi(nh\kappa), \tag{S6}$$

where

$$\varphi(k) = \frac{k}{2} \ln\left(\frac{1 + \frac{k}{2}}{1 - \frac{k}{2}}\right). \tag{S7}$$

The Taylor expansion $\varphi(k) = \frac{k^2}{2} + \frac{k^4}{24} + \cdots$ yields

$$\tilde{\mathcal{E}}(\kappa) = B_1 n \left(\frac{\kappa^2}{2} + \frac{(nh)^2}{24} \kappa^4 + \cdots\right). \tag{S8}$$

The first term in the expression above corresponds to the assumption that all layers have identical curvature κ. The subsequent terms bring in a non-linear correction that accounts for the fact that the different layers have different curvatures.

Analogous *Elastica* formulation: We assume the left/right mirror symmetry is preserved, such that only half of the stack is considered, with $S = 0$ as the point of indentation and $S = \ell$ as the contact point with the support, the equilibrium equation is found by requiring that the total energy is stationary. The energy in this problem consists of the bending energy $\mathcal{E}/2 = \int_{S=0}^{\ell} \tilde{\mathcal{E}} \mathrm{d}S$. The frictionless contact with the support is enforced through Lagrange multipliers F_1 and F_2 defined as positive, such that the quantity $\boldsymbol{F} = -F_1 \boldsymbol{e_1} + F_2/2 \boldsymbol{e_2}$ can be interpreted as the contact force with the support at $S = \ell$. Following a variational approach, we arrive at the following equilibrium equation:

$$\frac{nB_1 \theta''(S)}{\left(1 - \left(\frac{nh}{2}\theta'(S)\right)^2\right)^2} + (F_2/2 \cos\theta(S) + F_1 \sin\theta(S)) = 0, \tag{S9}$$

with the primes denoting differentiation with respect to S. The shape of the centerline $\boldsymbol{x}(S)$ is reconstructed from the solution $\theta(S)$ using $x_1'(S) = \cos(\theta)$ and $x_2'(S) = \sin(\theta)$. The symmetry of the problem imposes the following boundary condition on $S = 0$: $\theta(S = 0) = 0$ and $x_1(S = 0) = 0$. The displacement is controlled; *i.e.*, $x_2(S = 0) = -w_\circ$. The parameter ℓ is an unknown whose initial value $\ell = a$ increases as the deflection gets larger. We assume that the layers in the cantilevering portion of the setup extend sufficiently so that ℓ is below the physical half-length L of the plates. The part of the stack past the roller ($\ell \leq S \leq L$) does not deform, nor it contributes to the bending energy. At $S = \ell$, the tangent angle $\theta_\ell = \theta(S = \ell)$ is not known; it is effectively a free end and we enforce the boundary condition $\theta'(S = \ell) = 0$. The parameter ℓ is set by the condition of contact with the support, $x_1(S = \ell) = a - b \sin\theta_\ell$, $x_2(S = \ell) = b(\cos\theta_\ell - 1)$, with $b = b_0 + \frac{nh}{2}$ being the effective radius of the supports taking the thickness of the stack into account. The section of the plates beyond the contact point in $S = \ell$ follow a continuity condition in position and tangent. Finally, as the supports can freely rotate, the reaction force at $S = \ell$ must remain normal to the stack. The support creates a jump of $|\boldsymbol{F}|$ in the internal normal force of the stack. Being a normal force, it also imposes a relation between F_1 and F_2: $-F_1 \cos\theta_\ell + F_2/2 \sin\theta_\ell = 0$. A summary of the boundary-value problem is shown in Fig. S2. The solution of the problem is obtained numerically using a shooting method. The

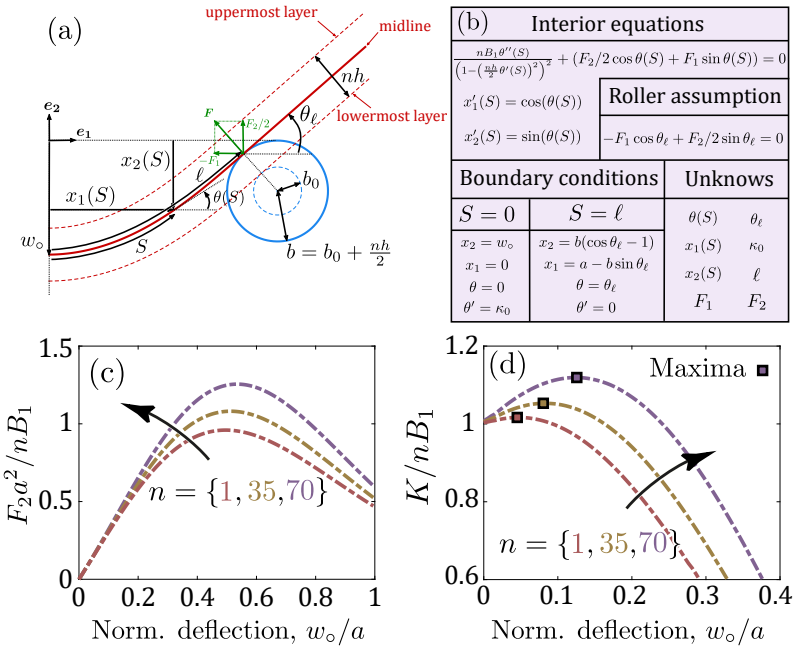

Supplementary Figure S2. (a) Schematic diagram of one half of a bent stack, illustrating the notations used. The centerline is shown in red (continuous red line) together with the uppermost and lowermost plates (dashed red lines). The physical extent of the roller is shown using a dashed blue circle, while the continuous blue line indicates the effective support interacting with the centerline. (b) Summary of the equations and variables. (c) Normalized load-deflection curves computed by solving the boundary-value problem summarized in (b) and detailed in the text. (d) Normalized incremental rigidity computed from the force curves in (c).

shooting method is implemented using Matlab (Matlab 2018b, Mathworks) and the function *ode45* to compute the solution of Eq. S9 expressed as a first order differential equation with 4 variables $Y = [\theta(S), \theta'(S), x_1(S), x_2(S)]$ and $Y' = [Y(2), \left(1 - \left(\frac{nh}{2}Y(2)\right)^2\right)^2 \times |\boldsymbol{F}| \left(\sin\theta_\ell \cos Y(1) + \cos\theta_\ell \sin Y(1)\right), \cos(Y(1)), \sin(Y(1))]$. For a given deflection and starting from $S = \ell$, the parameters $(\theta_\ell, \ell, |\boldsymbol{F}|)$ are varied using *fsolve* until the boundary conditions in $S = 0$ are verified.

S.III. Internal stress in the backbone solution

In this section, we provide a detailed justification for the elastic backbone (friction-less case), and we identify the microscopic stress, based on which, the expression for the power dissipated by friction is also obtained to first order in the friction coefficient.

Microscopic equations of equilibrium: We start with a detailed analysis of the elastic backbone model. We use two coordinate systems, (S, y) and $(\tilde{S}, y)$, where $\tilde{S}$ is the (Lagrangian) arc length along a plate, and S is the (non-Lagrangian) arclength of the projection of the current point onto the centerline in actual configuration. Each layer in the stack is in equilibrium. As a result, the shear and normal forces of the individual layers, denoted as $\tilde{T}$ and $\tilde{N}$ respectively, and their internal moment $\tilde{M}$ must satisfy the Kirchhoff equations for the equilibrium of elastic rods everywhere,

$$\begin{aligned} \frac{\partial \tilde{M}}{\partial \tilde{S}}(\tilde{S}, y) + \tilde{T}(\tilde{S}, y) &= 0 \\ \frac{\partial \tilde{N}}{\partial \tilde{S}}(\tilde{S}, y) - \tilde{\kappa}(\tilde{S}, y)\tilde{T}(\tilde{S}, y) &= 0 \\ \frac{\partial \tilde{T}}{\partial \tilde{S}}(\tilde{S}, y) + \tilde{\kappa}(\tilde{S}, y)\tilde{N}(\tilde{S}, y) + \tilde{p}_{\mathrm{n}}(\tilde{S}, y) &= 0 \end{aligned} \tag{S10}$$

Note that we follow the standard (but potentially confusing) convention whereby the normal force $\tilde{N}$ is along the tangent to the layer and the shear force $\tilde{T}$ is perpendicular to the layer. In this frictionless model, the loading applied on each layer is the *net* transverse force $\tilde{p}_{\mathrm{n}}\mathrm{d}\tilde{S}$; *i.e.*, the balance of transverse forces applied by the adjacent layers.

Microscopic shear force: Along a given layer, the transverse coordinate y is constant. The shear force $\tilde{T}(\tilde{S},y)$ can be found by combining the balance of moments in Eq. (S10), with the constitutive law $\tilde{M}=B_1\tilde{\kappa}$ and using the expressions of the plate curvature $\tilde{\kappa}(\tilde{S},y)$ in terms of the centerline curvature $\kappa(S)$ from Eq. (S4), as well as $\mathrm{d}\tilde{S}$ from Eq. (S3):

$$\begin{aligned}\tilde{T} &= -\tfrac{\partial\tilde{M}}{\partial\tilde{S}}\\ &= -\tfrac{\partial M}{\partial S}\tfrac{1}{1-\kappa y}\\ &= -\tfrac{B_1}{1-\kappa y}\tfrac{\partial\tilde{\kappa}}{\partial S}\\ &= -\tfrac{B_1}{1-\kappa y}\tfrac{\partial}{\partial S}\left(\tfrac{\kappa}{1-\kappa y}\right)\\ &= -\tfrac{B_1}{1-\kappa y}\tfrac{\partial\kappa}{\partial S}\left(\tfrac{1}{1-\kappa y}+\tfrac{\kappa y}{(1-\kappa y)^2}\right)\\ &= -\tfrac{B_1}{(1-\kappa y)^3}\tfrac{\mathrm{d}\kappa}{\mathrm{d}S}.\end{aligned} \tag{S11}$$

Microscopic normal force: In view of the longitudinal balance of forces in Eq. (S10), the normal force satisfies:

$$\begin{aligned}\tfrac{\partial\tilde{N}}{\partial S}(S,y) &= \tfrac{\partial\tilde{N}}{\partial\tilde{S}}(1-\kappa(S)y)\\ &= \tilde{\kappa}\tilde{T}(1-\kappa(S)y)\\ &= \kappa\tilde{T}\\ &= -\tfrac{B_1\kappa}{(1-\kappa y)^3}\tfrac{\mathrm{d}\kappa}{\mathrm{d}S}\\ &= -\tfrac{B_1}{y^2}\tfrac{\kappa y}{(1-\kappa y)^3}\left(y\tfrac{\mathrm{d}\kappa}{\mathrm{d}S}\right)\\ &= \tfrac{B_1}{y^2}\tfrac{\partial\psi(\kappa(S)y)}{\partial S}\\ &= \tfrac{\partial}{\partial S}\left[\tfrac{B_1}{y^2}\psi(\kappa(S)y)\right],\end{aligned}$$

where we have introduced the auxiliary function $\psi(k)=-\frac{k^2}{2(1-k)^2}$, with deriviative $\psi'(k)=-\frac{k}{(1-k)^3}$.

By integrating $\partial\tilde{N}/\partial S$ we find the normal force as

$$\begin{aligned}\tilde{N}(S,y) &= \tfrac{B_1}{y^2}\psi(\kappa y)+\mathrm{Cte}(y)\\ &= -\tfrac{B_1\kappa^2}{2(1-\kappa y)^2}+\mathrm{Cte}(y)\end{aligned}$$

The integration we just did cannot be carried out across the points of discontinuity. As a result, the constant of integration $\mathrm{Cte}(y)$ may be different in each of the regions separated by the point-like forces. In particular, in the half-domain $0\leqslant S\leqslant L$, there is *a priori* one function $\mathrm{Cte}(y)$ in the interval $0\leqslant S\leqslant\ell$ and a different function $\mathrm{Cte}(y)$ in the interval $\ell\leqslant S\leqslant L$:

- Beyond the supports ($\leqslant S\leqslant\ell$), the plates are underformed so $\kappa=0$, and $\tilde{N}(S,y)=\mathrm{Cte}(y)$. The free-boundary condition at $S=L$ sets $\mathrm{Cte}(y)=0$ and, hence, $\tilde{N}(S,y)=0$;
- At the roller ($S=\ell$), the applied force is purely transverse, implying that the normal force $\tilde{N}$ is actually continuous, $[\![\tilde{N}]\!]_\ell=\tilde{N}(\ell^+,y)-\tilde{N}(\ell^-,y)=-\tilde{N}(\ell^-,y)=0$. Since the moment is zero at $S=\ell^-$, so is the curvature, $\kappa(\ell^-)=0$; then $\tilde{N}(\ell^-,y)=0$ implies $\mathrm{Cte}(y)=0$.

We have just shown that the quantity $\mathrm{Cte}(y)$ is zero everywhere; *i.e.*,

$$\tilde{N}(S,y)=-\frac{B_1}{2}\left(\frac{\kappa}{1-\kappa y}\right)^2.$$

Normal stress – regular part: Let us now evaluate the normal forces applied from the neighbors to a given layer $\tilde{p}_\mathrm{n}\mathrm{d}\tilde{S}$ for $S<\ell$, for which we will use transverse equilibrium,

$$\begin{aligned}\tilde{p}_\mathrm{n}\mathrm{d}\tilde{S} &= \tilde{p}_\mathrm{n}(1-\kappa y)\mathrm{d}S\\ &= -\left(\tfrac{\partial\tilde{T}}{\partial\tilde{S}}+\tilde{\kappa}\tilde{N}\right)(1-\kappa y)\mathrm{d}S\\ &= -\left(\tfrac{\partial\tilde{T}}{\partial S}+\kappa\tilde{N}\right)\mathrm{d}S\\ &= B_1\left(\tfrac{\partial}{\partial S}\left(\tfrac{1}{(1-\kappa y)^3}\tfrac{\mathrm{d}\kappa}{\mathrm{d}S}\right)+\kappa\tfrac{1}{2}\left(\tfrac{\kappa}{1-y\kappa}\right)^2\right)\mathrm{d}S\\ &= B_1\left(\tfrac{1}{2}\tfrac{\kappa^3}{(1-y\kappa)^2}+\tfrac{3y}{(1-\kappa y)^4}\left(\tfrac{\mathrm{d}\kappa}{\mathrm{d}S}\right)^2+\tfrac{1}{(1-\kappa y)^3}\tfrac{\mathrm{d}^2\kappa}{\mathrm{d}S^2}\right)\mathrm{d}S.\end{aligned}$$

In the main text, we have defined $\Sigma(S,y)$ as the normal stress at the plate-plate interfaces. The normal force applied by the plate above (respectively, below) the plate having mean coordinate y, over an interface element with length $\mathrm{d}\tilde{S}$, is therefore $-\Sigma(S,y+h/2)\mathrm{d}\tilde{S}$ (respectively, $+\Sigma(S,y-h/2)\mathrm{d}\tilde{S}$). The net force experienced by the plate from the adjacent plates is therefore $\tilde{p}_\mathrm{n}\mathrm{d}\tilde{S} = h\frac{\partial(\Sigma\mathrm{d}\tilde{S})}{\partial y}$, which we can rewrite as

$$h\frac{\partial(\Sigma(1-\kappa y))}{\partial y} = \tilde{p}_\mathrm{n}(1-\kappa y). \tag{S12}$$

This equation can be integrated with respect to y, using the free boundary conditions at top and bottom of the stack $\Sigma(S,\pm\frac{nh}{2})=0$; this yields the normal stress in the elastic backbone solution as

$$\Sigma(S,y) = \frac{1}{h(1-\kappa(S)y)}\int_{-\frac{nh}{2}}^{y} B_1\left(\frac{1}{2}\frac{\kappa^3(S)}{(1-\kappa(S)\tilde{y})^2} + \frac{3\tilde{y}}{(1-\kappa(S)\tilde{y})^4}\left(\frac{\mathrm{d}\kappa}{\mathrm{d}S}\right)^2 + \frac{1}{(1-\kappa(S)\tilde{y})^3}\frac{\mathrm{d}^2\kappa}{\mathrm{d}S^2}\right)\mathrm{d}\tilde{y}. \tag{S13}$$

One can check that the stress-free condition at the top of the stack $\Sigma(S,y=\frac{nh}{2})=0$ is automatically satisfied, even if it has not been enforced.

The normal stress $\Sigma(S,y)$ is evaluated and represented in Fig. S3(a). We observe that the pressure is always negative, meaning that the plates are pressing against each other.

Normal stress – singular contribution at the rollers: The expression in Eq. (S13) for the normal stress is valid away from the points $S\in\{-\ell,0,\ell\}$, where point-like forces are applied. We do not need to derive the singular normal stress at the point of indentation $S=0$, since the sliding velocity of the plates is zero there by symmetry, implying that there is no frictional dissipation.

We proceed to derive the singular (Dirac-like) contribution of the internal stress at the roller $S=\ell$. The other roller $S=-\ell$ is treated similarly, by symmetry. At $S=\ell$, the point-like force applied by the roller induces a point-like net normal force $\tilde{p}_\mathrm{n}^D$ applied to each plate, leading to the following balance of forces and moments,

$$[\![\tilde{T}]\!]_\ell + \tilde{p}_\mathrm{n}^D = 0, \quad [\![\tilde{N}]\!]_\ell = 0, \quad [\![\tilde{M}]\!]_\ell = 0. \tag{S14}$$

where $[\![f]\!]_\ell = f(y,\ell^+) - f(y,\ell^-)$ denotes the discontinuity of a function f across $S=\ell$. The equation $[\![\tilde{N}]\!]_\ell=0$ has already been used to determine $\tilde{N}$. The equation $[\![\tilde{M}]\!]_\ell=0$ has been used to show that the curvature is continuous across $S=\ell$, which motivates the boundary condition $\kappa(\ell^-)=\theta'(\ell^-)=0$ used in the boundary value problem of the elastic backbone.

We insert the expression of $\tilde{T}$ from Eq. (S11) into the balance of normal forces $[\![\tilde{T}]\!]_\ell+\tilde{p}_\mathrm{n}^D=0$; noting that $\frac{\mathrm{d}\kappa}{\mathrm{d}S}(\ell^+)=0$, as the plates remain straight for $S>\ell$, we obtain:

$$B_1\frac{\mathrm{d}\kappa}{\mathrm{d}S}(\ell^-) + \tilde{p}_\mathrm{n}^D = 0 \tag{S15}$$

By the same argument as earlier, the Dirac-like contribution to the normal stress $\Sigma^D(y)$ at $S=\ell$ satisfies the differential equation

$$h\frac{\partial\Sigma^D}{\partial y} = \tilde{p}_\mathrm{n}^D$$

as well as the boundary conditions

$$\Sigma^D\left(-\frac{nh}{2}\right) = -|\boldsymbol{F}| \quad 2\,\mathrm{em}\Sigma^D\left(+\frac{nh}{2}\right) = 0$$

where $\boldsymbol{F}$ is the point-like force applied by the roller from below. The solution is found by integration as

$$\Sigma^D(y) = -\frac{1}{h}\int_y^{+\frac{nh}{2}} \tilde{p}_\mathrm{n}^D\mathrm{d}\tilde{y} = \frac{1}{h}B_1\frac{\mathrm{d}\kappa}{\mathrm{d}S}(\ell^-)\left(\frac{nh}{2}-y\right). \tag{S16}$$

The constant of integration warrants the equilibrium on the topmost interface. The equilibrium of the bottommost interface yields

$$nB_1\frac{\mathrm{d}\kappa}{\mathrm{d}S}(\ell^-) = -|\boldsymbol{F}|. \tag{S17}$$

This equation can be interpreted as a balance of transverse force for the one-dimensional model across the singularity (details not shown). In view of this, the singular contribution to the transverse stress at $S = \ell$ can be rewritten as

$$\Sigma^D(y) = -|\boldsymbol{F}| \left(\frac{1}{2} - \frac{y}{nh} \right). \tag{S18}$$

Sliding velocity: We define the sliding displacement as

$$u(y, S) = \tilde{S}(y, S) - S,$$

which satisfies

$$\frac{\partial u}{\partial S} = \frac{\partial \tilde{S}}{\partial S} - 1 = -\kappa(S) y, \tag{S19}$$

and, hence,

$$u(y, S) = -y\theta(S). \tag{S20}$$

The relative displacement at an interface therefore reads

$$\delta(y, S) = \tilde{S}\left(y + \frac{h}{2}, S\right) - \tilde{S}\left(y - \frac{h}{2}, S\right) = u\left(y + \frac{h}{2}, S\right) - u\left(y - \frac{h}{2}, S\right) = h\frac{\partial u}{\partial y}(u, S) = -h\theta(S). \tag{S21}$$

The time derivative of this expression yields the relative sliding velocity:

$$\dot{\delta}(y, S) = -h\dot{\theta}(S). \tag{S22}$$

Perturbative expression for the power dissipated by frictional forces: Throughout our study, friction is treated as a perturbation; we assume that friction does not significantly affect the microscopic stress in the stack, nor the sliding velocities at the interfaces. We use an Amontons-Coulomb friction law between the plates, which yields the tangent stress at the interfaces between plates as $\mu\Sigma$, where μ is the friction coefficient. There are also singular (Dirac-like) tangent force at the points with coordinates $S \in \{-\ell, 0, \ell\}$ on each of the interfaces; that corresponding to $S = \ell$ reads $\mu\Sigma^D$. Now, we seek to compute the power dissipated by friction in the entire stack $\mathcal{P}_\mu$, for which we have to first consider two separate contributions, $\mathcal{P}_1$ and $\mathcal{P}_2$, which are detailed next.

The power $\mathcal{P}_1$ dissipated by friction away from the singular points $S \in \{-\ell, 0, \ell\}$ is the integral over all plate-plate interfaces of $\mu\Sigma$ times the sliding velocity $\dot{\delta}$:

$$\mathcal{P}_1 = \mu \int_{-L}^{L} \mathrm{d}S \int_{-\frac{nh}{2}}^{+\frac{nh}{2}} h|\dot{\theta}(S)|(-\Sigma(S, y))\frac{\mathrm{d}y}{h} \tag{S23}$$

where we assume that $\Sigma(S, y) < 0$ everywhere, as we checked. In this expression, there is an integral $\int \cdots \mathrm{d}S$ along the interfaces, and an integral $\int \cdots \frac{\mathrm{d}y}{h}$ which serves as a continuous approximation to the sum over all interfaces. Performing the integration in Eq. (S23) with respect to the transverse variable y, by (i) omitting the regions $|S| > \ell$ where the normal stress is zero, (ii) identifying the quantity $Q(S) = \int_{-\frac{nh}{2}}^{+\frac{nh}{2}} (-\Sigma(S, y))\mathrm{d}y$ defined in the main text, and (ii) limiting the integration to the domain $S \geqslant 0$ by symmetry, yields

$$\mathcal{P}_1 = 2\mu \int_0^\ell Q(S)|\dot{\theta}(S)|\mathrm{d}S.$$

The power dissipated by friction caused by the Dirac-like contribution at $S = 0$ is zero, since the sliding velocity is zero there, $\dot{\delta}(0, S) = 0$.

The power $\mathcal{P}_2$ dissipated by friction caused by the Dirac-like contribution at $S = \ell$ writes, by a similar argument, as

$$\mathcal{P}_2 = \mu \int_{-\frac{nh}{2}}^{+\frac{nh}{2}} h|\dot{\theta}(\ell)|(-\Sigma^D(y))\frac{\mathrm{d}y}{h}.$$

Using Eq. (S18), we can calculate the intregral as

$$\mathcal{P}_2 = \mu hn|\dot{\theta}(\ell)|\frac{|\boldsymbol{F}|}{2}. \tag{S24}$$

For a given value for the friction coefficient μ, $\mathcal{P}_1$ appears to be somewhat smaller than (but still comparable to) $\mathcal{P}_2$, see Fig. S3(b). Finally, the power dissipated by friction in the entire stack is

$$\mathcal{P}_\mu = 2\mathcal{P}_2 + \mathcal{P}_1, \tag{S25}$$

where the factor 2 is because there are two rollers. This is the expression used in the main text.

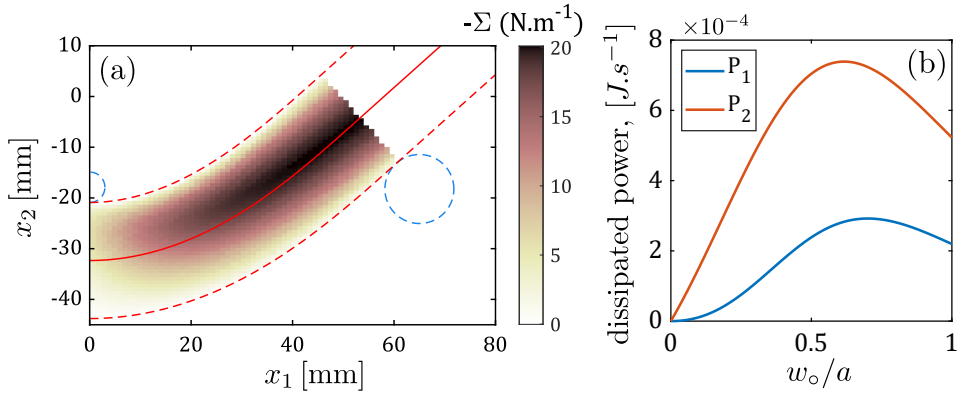

Supplementary Figure S3. (a) Regular part of the normal stress in the stack $\Sigma(S, y)$, at an indentation level of $w_0/a = 0.5$. Σ does not include the singular contributions of the indenter and the rollers. (b) Comparison between the power dissipated away from the point of contact ($S < \ell$), $\mathcal{P}_1$ and at the contact point $\mathcal{P}_2$. For both (a) and (b) the following parameters have been used: $a = 65\,\mathrm{mm}$, $h = 0.286\,\mathrm{mm}$, $B_1 = 1.76.10^{-4}\,\mathrm{N.m^2}$, $b_0 = 6.8\,\mathrm{mm}$, $n = 80$, $\dot{w_\circ} = 1\,\mathrm{mm.s^{-1}}$ and $\mu = 0.52$.

S.IV. The case of small deflections

In this section, we consider the limit where the deflection is small, $w_\circ/a \ll 1$, and the stack is overall slender, $nh/a \ll 1$.

We start with a linear analysis of the backbone solution. In this limit, the stack's centerline can be analyzed using the approximations $\cos\theta = 1$, $\sin\theta = \theta$ and $\ell = a$. The linearized equilibrium equations in the transverse direction write

$$nB_1 \frac{\mathrm{d}^2\theta}{\mathrm{d}S^2} + \frac{F_2}{2} = 0 \quad \frac{\mathrm{d}x_2}{\mathrm{d}S} = \theta,$$

with the boundary conditions: $x_2(0) = -w_\circ$, $x_2(a) = 0$, $\theta(0) = 0$ and $\frac{\mathrm{d}\theta}{\mathrm{d}S}(a) = 0$. This equivalent, linear beam problem, with a bending stiffness nB_1, is solved as

$$\begin{aligned} \theta_{\mathrm{bb}}(S) &= \tfrac{F_2 a^2}{2nB_1}\left(\tfrac{S}{a} - \tfrac{1}{2}\left(\tfrac{S}{a}\right)^2\right) \\ x_{2,\mathrm{bb}}(S) &= \tfrac{F_2 a^3}{4nB_1}\left(-\left(1 - \left(\tfrac{S}{a}\right)^2\right) + \tfrac{1}{3}\left(1 - \left(\tfrac{S}{a}\right)^3\right)\right) \end{aligned} \tag{S26}$$

This result implies the linear indentation law $F_{2,\mathrm{bb}} = \frac{6nB_1}{a^3} w_\circ$. Consequently, the elastic energy of the stack writes as $\mathcal{E}(w_\circ) = \frac{3nB_1}{a^3} w_\circ^2$, from which we recover the incremental rigidity $K_{\mathrm{bb}}(w_\circ) = \frac{a^3}{6}\frac{\mathrm{d}F_{2,\mathrm{bb}}}{\mathrm{d}w_\circ} = nB_1$ announced in the main text.

In the limit $nh/a \ll 1$, all the plates have the same shape, given by the centerline plus a constant vertical offset; *i.e.*, $\tilde{\boldsymbol{x}}(S, y) = S\boldsymbol{e}_1 + (x_{2,\mathrm{bb}}(S) + y)\,\boldsymbol{e}_2$, with $\tilde{S} = S$ in this linearized setting. Inserting this result into the local equations of equilibrium for the individual layers, Eq. (S10), one finds $\tilde{p}_\mathrm{n} = 0$, meaning that away from the indentation point and from the rollers, $S \notin \{-\ell, 0, \ell\}$, each layer is in equilibrium without any applied force. In view of Eq. (S12), the normal stress $\Sigma(S, y)$ is independent of y. With the stress-free boundary conditions on the uppermost and lowermost faces, we have that

$$\Sigma(S, y) = 0,$$

in the linear regime. In view of Eq. (S23), this result implies $\mathcal{P}_1 = 0$; *i.e.*, for small friction and small deflection, dissipation occurs dominantly at the rollers, at $S = \pm\ell$.

Using Eqs. (S24–S25), we find that the power dissipated by friction can be estimated based on the elastic backbone solution as $\mathcal{P}_\mu = \frac{\mu nh|\boldsymbol{F}|}{2}|\dot{\theta}_{\mathrm{bb}}(a)|$. In the linear regime, $\boldsymbol{F}$ can be approximated as $F_2/2\boldsymbol{e}_2$; *i.e.*,

$$\mathcal{P}_\mu = \frac{\mu nhF_2}{2}|\dot{\theta}_{\mathrm{bb}}(a)| \tag{S27}$$

We know that $F_{2,\mathrm{bb}} = \frac{6nB_1}{a^3} w_\circ$, and Eq. (S26) shows that $\theta_{\mathrm{bb}}(a) = \frac{F_{2,\mathrm{bb}} a^2}{4nB_1} = \frac{3}{2a} w_\circ$. Inserting this result into the right-hand side of Eq. (S27), we find

$$\mathcal{P}_\mu = \frac{9}{2}\frac{\mu hn^2 B_1}{a^4} w_\circ |\dot{w_\circ}|.$$

The expression of the indentation force $F_2^{\pm}(w_\circ)$ can now be derived using Eq (4) from the main text, while taking into account the frictional dissipated energy, as

$$F_2^{\pm} = \frac{6}{a^2} n B_1 \left(1 \pm \frac{3}{4}\mu n \frac{h}{a}\right) \frac{w_\circ}{a}, \tag{S28}$$

with the + sign for loading and − for unloading. Therefore, our linear theory predicts an apparent, incremental (scaled) stiffness

$$K_{\text{lin}} = n B_1 \left(1 \pm \frac{3}{4}\mu n \frac{h}{a}\right), \tag{S29}$$

where friction causes an apparent stiffening upon loading and an apparent softening upon unloading.

The expression of F_2 for loading and unloading in Eq. (S28) yields the following prediction for the energy dissipated during one cycle:

$$\begin{aligned} D_{\text{lin}} &= \int_0^{w_\circ^{max}} F_2^{+}\,\mathrm{d}w_\circ - \int_0^{w_\circ^{max}} F_2^{-}\,\mathrm{d}w_\circ \\ &= \frac{9\mu B_1 h}{2a^2}\left(n\frac{w_\circ^{\max}}{a}\right)^2, \end{aligned}$$

which is plotted as the dashed line in Fig. 3(b) of the main text.

S.V. Measure of the effective friction coefficient μ

In Eq. (S29) above, we wrote the bending rigidity of the stack, K_{lin}, for the linear case. We extrapolate this prediction to the frictional nonlinear regime by applying the same corrective factor $\left(1 \pm \frac{3}{4}\mu n \frac{h}{a}\right)$ to the friction-less, geometrically nonlinear prediction for the maximum incremental stiffness (elastic backbone) $K_{\text{m,bb}} = \max_{w_\circ}(K_{\text{bb}})$ where $K_{\text{bb}}(w_\circ) = \frac{a^3}{6}\,\mathrm{d}F_{2,\text{bb}}/\mathrm{d}w_\circ$ (see Fig. S4a):

$$K_{\text{m}}^{\pm} = K_{\text{m,bb}} \cdot \left(1 \pm \frac{3}{4}\mu n \frac{h}{a}\right). \tag{S30}$$

The increase in apparent rigidity due to friction $\pm(K_{\text{m}}^{\pm}/K_{\text{m,bb}} - 1) = \frac{3}{4}\mu n \frac{h}{a}$ should therefore depend linearly on n, see Fig. S4(b). This prediction is indeed verified by the experimental data for both loading and unloading, which enables us to extract the friction coefficient as $\mu = 0.52 \pm 0.03$.

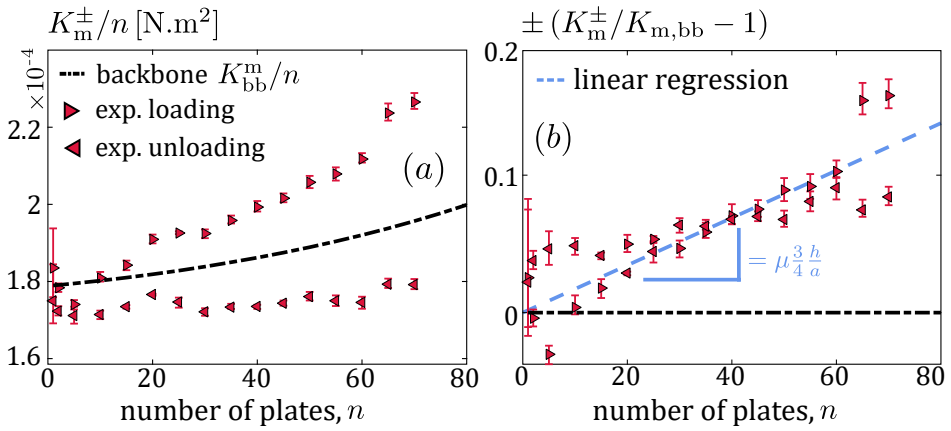

Supplementary Figure S4. Extraction of the friction coefficient from experimental data. (a) Scaled maximum stiffness $K_{\text{m}}^{\pm}/n$ as a function of n, for loading ($\triangleright$) and unloading ($\triangleleft$). The dashed-dotted curve is the prediction from the elastic backbone solution. (b) Increase in apparent rigidity due to friction: the slope from the linear regression versus n (dashed blue line) provides a measure of the friction coefficient μ.